UC Irvine
UC Irvine Previously Published Works

Title
A corrosion study of Ag–Al intermetallic compounds in chlorine-containing epoxy molding compounds

Permalink
https://escholarship.org/uc/item/78b4m6sh

Journal
Journal of Materials Science: Materials in Electronics, 28(20)

ISSN
0957-4522

Authors
Fu, Shao-Wei
Lee, Chin C

Publication Date
2017-10-01

DOI
10.1007/s10854-017-7467-4

Peer reviewed

eScholarship.org Powered by the California Digital Library
University of California

J Mater Sci: Mater Electron
DOI 10.1007/s10854-017-7467-4

A corrosion study of Ag–Al intermetallic compounds in chlorine-containing epoxy molding compounds

Shao-Wei Fu[1,2] · Chin C. Lee[1,2]

Received: 13 April 2017 / Accepted: 3 July 2017
© Springer Science+Business Media, LLC 2017

Abstract Typical epoxy molding compounds (EMC) contain chlorine ions that cause silver wire-bond failures under highly accelerated temperature/humidity stress test (HAST). To understand the corrosion mechanisms, experiments were designed to emulate the HAST environment and conditions and performed. Specifically, Ag–Al joints, Ag, Al, Ag_3Al, and Ag_2Al samples were encapsulated in chlorine-containing EMC, respectively, and went through HAST. EMC with high chlorine content (1000 ppm) was chosen to accelerate the corrosion rate and shorten experiment time. The experimental results show that chlorine-induced corrosion occurs only on Ag_3Al and Ag_2Al compounds. It does not occur on Ag or Al samples. The corrosion rates of bulk Ag_3Al and Ag_2Al disks were measured under HAST up to 125 h. The corrosion rate of Ag_3Al is twice of that of Ag_2Al, meaning that Ag_2Al is more resistant to corrosion. Careful evaluations reveal that the corrosion is caused by both moisture and Cl^- ions. Microstructures, compositions, and phases of corroded regions were examined in details. In the corroded regions, Ag_3Al and Ag_2Al compounds disintegrate into aluminum oxide pieces and dispersed Ag precipitates with voids and cracks. The chlorines detected near voids and cracks suggest formation of aluminum chloride as an intermediate product that is hydrolyzed into aluminum oxide. A corrosion chemical model is proposed to establish the reactions of Ag_3Al and Ag_2Al compounds with chlorine-containing EMC. New information obtained in this research can help the search of new processes and techniques to counter or reduce the chlorine-induced corrosion of devices and packages. The corrosion test method presented may possibly become an acceptable test standard to consider.

✉ Shao-Wei Fu
shaoweif@uci.edu

[1] Electrical Engineering and Computer Science, University of California, Irvine, CA 92697-2660, USA

[2] Materials and Manufacturing Technology, University of California, Irvine, CA 92697-2660, USA

1 Introduction

Wire bonding technique has been extensively used to interconnect chips and substrates of microelectronic packages [1–3]. Gold (Au) wire had been most popular for decades, providing excellent workability and stable chemical properties [4, 5]. However, the rising gold price has motivated the packaging industry to look for alternative wire materials such as silver (Ag) and copper (Cu) [5–9]. Recently, several packaging companies have bonded Cu wires on aluminum (Al) bond-pads in production. The reaction on Cu/Al interface and Cu wire-bond reliability have been reported [5, 6]. Since Cu wires get oxidized easily and are harder than Au and Ag alloy wires, the process window of Cu wire bonding is narrower. Special bonding equipment are usually needed. Other issues on Cu wire-bonds are splashing on Al pads and Si chip cratering [8].

Most recently, Ag alloy wires have been chosen as a possible alternative [9, 10]. Compared to Cu wires, Ag alloy wires have lower oxidation rate and higher ductility. It had been reported that Ag alloy wire bonding exhibits wider process window and causes less Al pad splash and silicon damage [11]. In choosing a wire material, one important thing to consider is how it bonds to the Al pads [12, 13]. Several research works have shown that the bonding on the Ag–Al interface is caused by intermetallic compound (IMC) formation [14–16]. Based on the Ag–Al phase diagrams [17, 18] and experiment results, the main IMCs are

Published online: 13 July 2017

Ag_3Al and Ag_2Al [15–18]. Reliability of Ag alloy wire-bonds has been evaluated under high temperature and high humidity test conditions [11, 13–16]. In high temperature storage test (HTS), Ag alloy wire-bonds pass industrial reliability standard [11, 14, 15]. Microstructures of Ag alloy wire-bonds exhibit homogenous IMC growth without cracks or Kirkendall void formation. No electrical degradation is detected. Under humidity storage test conditions, wire-bond failure rate increases [13, 16, 19]. In Highly Accelerated temperature/humidity Stress Test (HAST) and Pressure Cooker Test (PCT), cracks and voids incur at the Ag/Al bonding interface, causing wire-bond failure. Moisture-induced corrosion at the Ag/Al bonding interface seems to be the root cause of this failure. Similar corrosion effect is also observed in Au–Al and Cu–Al wire-bonds [20–23]. The corrosion is strongly associated with halogen content, such as chlorine (Cl), in the epoxy molding compounds (EMCs). However, the corrosion mechanism of Ag–Al wire-bonds is still unclear.

In this research, to find out how Ag–Al wire-bonds are corroded, experiments are designed to emulate the wire-bond environment and conditions. As a first step, instead of using actual wire-bonds, bulk Ag–Al joints are produced with enough Ag_3Al and Ag_2Al volume for HAST and corrosion measurements. Since Ag–Al wire-bonds consist of Ag alloy wire, Ag_3Al and Ag_2Al on the interface, and the Al pad, corrosion experiment of each component with EMC is conducted with HAST for 125 h. The experimental results show that corrosion occurs with Ag_3Al and Ag_2Al but not with Ag or Al. A corrosion chemical model is proposed to establish the reactions of Ag_3Al and Ag_2Al compounds with chlorine-containing EMC.

2 Experimental design and procedures

A typical wire bond is too small to produce enough corrosion volume for analysis. To emulate Ag–Al wire-bonds for the purpose of corrosion study, Ag–Al joints are prepared by bonding Ag disks to Al substrates using the solid-state bonding process. The bonding process was performed at 450 °C with a 1000 psi (6.89 MPa) static pressure for 10 min in 0.1 Torr vacuum. Subsequently, the Ag–Al joints are annealed at 300 °C for 100 h to grow enough Ag–Al IMC layer. The resulting Ag–Al joints are molded in EMC for HAST. The test conditions are 130 °C and 85% relative humidity (RH) without applied bias. High chlorine content (1000 ppm) is added to the EMC to accelerate the corrosion reaction and to shorten the experiment time. The chlorine content is controlled by the amount of hydrolyzable chloride (3-chloro-1-propanol) added into the EMC.

To measure corrosion rates, corrosion experiments of bulk Ag, Ag_3Al, Ag_2Al and Al disks with EMC are conducted, respectively. To produce Ag_3Al and Ag_2Al disks, single-phase Ag_3Al and Ag_2Al ingots are grown by a casting method. Ag-35 at.% Al mixture and Ag-22 at.% Al mixture are, respectively, loaded in quartz tubes and sealed in vacuum to form capsules. The capsules are brought to 1273 K (1000 °C) and stay at this temperature for 5 h. This is followed by water quenching to room temperature and solid-state annealing at 473 K (200 °C) for 750 h. X-ray diffraction (XRD) analysis is used to confirm that these ingots are indeed single phase Ag_3Al and Ag_2Al, respectively. The ingots are cut into disks and polished for corrosion experiments. The bulk disks are encapsulated in EMC and tested at 130 °C and 85% RH (HAST) for 25, 50 and 125 h, respectively.

To study the corrosion reactions, the encapsulating EMC samples are cut in cross-section and fine polished for optical microscopy (OM) inspection and scanning electron microscopy/energy dispersive X-ray spectroscopy (SEM/EDX, FEI Philips XL-30, FEG SEM) examinations in back-scattered electron (BSE) mode.

3 Results and discussion

As presented in previous section, Ag–Al joints are prepared by bonding Ag disks to Al substrates using solid-state bonding process. After annealing at 300 °C for 100 h to grow IMC, the resulting Ag–Al joints are molded in EMC. EMC with high chlorine content (1000 ppm) is used to accelerate corrosion reactions. The molded Ag–Al joints are tested by HAST (130 °C, 85% RH) for 100 h. Fig. 1 displays the cross section optical microscopy and back-scattered electron images of representative samples. Before HAST, a 20 µm thick Ag–Al IMC layer is clearly observed in Fig. 1a, b. Based on compositions measured by EDX analysis, shown in Table 1, the IMC layer consists of both Ag_3Al and Ag_2Al. Figure 1c and d exhibit a sample after HAST. As shown in the optical image, Fig. 1c, corrosion mainly occurred in the IMC area, and no reaction was observed on Ag or Al. The IMC layer had turned black with continuous cracks. Corrosion and cracks propagated through the entire IMC layer to break it down to small particles and fragments. This makes it difficult to achieve nice polishing on cross section surfaces. The particles and fragments got onto the Ag and Al areas during the polishing process, causing scratches on the sample cross section, as exhibited in Fig. 1c. In the corroded IMC region, EDX analysis did not pick up compositions associated with Ag_3Al and Ag_2Al compounds, indicating that the original IMC layer had been completely disintegrated. On the corroded region, EDX analysis picked up elements Ag, Al, O and Cl, as shown in Table 1. From EDX results, the corrosion in Ag–Al joints was caused by the oxidation of the

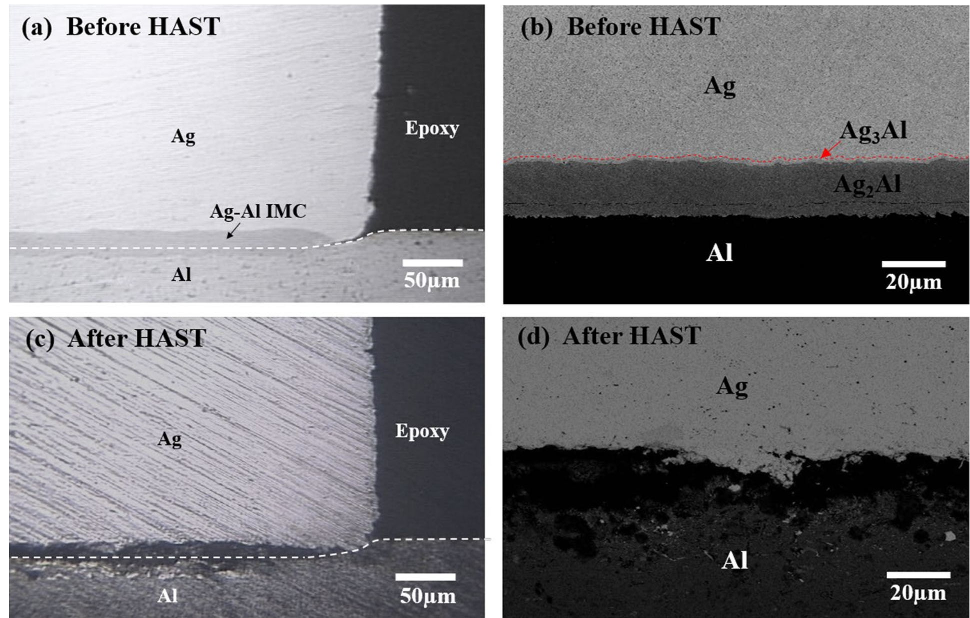

Fig. 1 Cross-sectional images of the Ag–Al joints molded in EMC: **a** optical microscopy image before HAST, **b** back-scattered electron image before HAST, **c** optical image after HAST, **d** back-scattered electron image after HAST

Table 1 Compositions (at.%) of intermetallic compound layer in the Ag–Al joint molded in EMC before and after HAST

	Ag	Al	O	Cl	Remark
Before HAST	78.8	21.2	0.0	0.0	Ag_3Al
	66.2	33.8	0.0	0.0	Ag_2Al
After HAST	25.0	33.9	58.9	1.2	Corrosion region

IMC region in the presence of moisture and chlorine. At high humidity ambient, water vapor can penetrate into EMC and react with hydrolyzable chloride in EMC to produce Cl^- ions [24, 25]. Water and Cl^- ions can diffuse and reach the Ag/Al interface and initiate the IMC corrosion. As water and Cl^- ions penetrate through the corroded IMC region, the corrosion action can continue towards the center of the Ag–Al joint interface.

The results reported above have clearly indicated that in Ag–Al joints, corrosion by Cl^- ions mainly occur at the Ag–Al IMC region. To find out the IMC corrosion rate and investigate the microstructures and compositions of the corroded IMC region, reaction experiments with bulk Ag_3Al and Ag_2Al disks were designed and performed. First, single-phase Ag_3Al and Ag_2Al ingots were produced. Figure 2 displays the XRD spectra and EDX analysis compositions of the Ag_3Al and Ag_2Al ingots. For the Ag_3Al sample, all XRD peaks belong to Ag_3Al lattice that has cubic structure (A13, β-Mn type). For the Ag_2Al sample, all peaks belong to Ag_2Al lattice that has hexagonal structure (A3, Mg type). The Ag_3Al and Ag_2Al ingots were cut into disk samples and polished. The polished samples were encapsulated in EMC

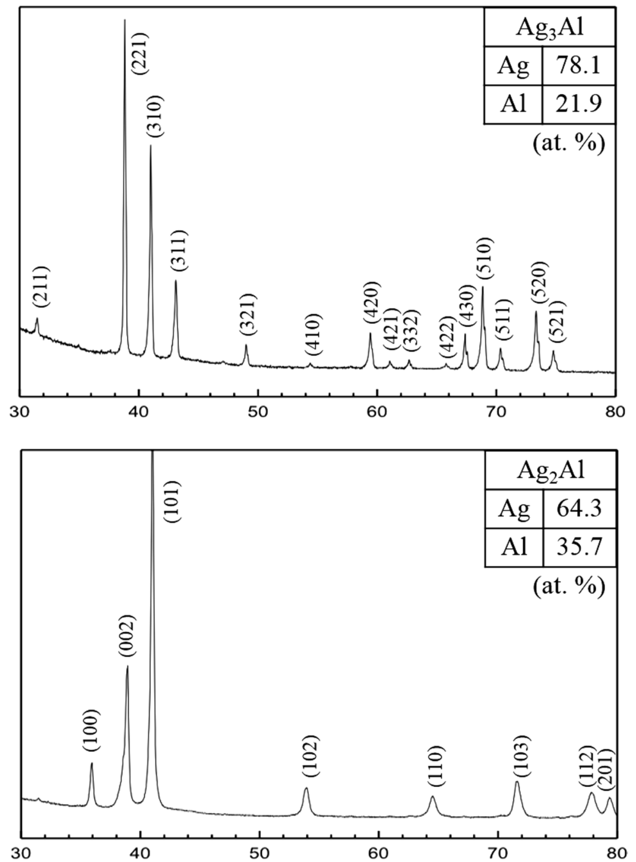

Fig. 2 EDX composition analysis results and the XRD spectrum of the Ag_3Al and Ag_2Al intermetallic alloys

and tested by HAST (130 °C, 85% RH) for 25, 50, and 125 h, respectively. Figure 3 exhibits the cross-section SEM back-scattered electron images of molded Ag_3Al and Ag_2Al samples after HAST for different times. It is clearly observed that corrosion occurred on both Ag_3Al and Ag_2Al disks under HAST. The images show continuous corrosion regions of depth up to 100 µm on both Ag_3Al and Ag_2Al disks. An important fact to confirm is whether Ag or Al can be corroded by chlorine-containing EMC. Reaction experiments with Ag and Al disks were performed under the same HAST conditions. As presented in Fig. 4, the cross-section SEM image shows no detectable corrosion on the bulk Ag sample encapsulated in chlorine-containing EMC after HAST for 125 h. The same is true for the bulk Al sample. The above results demonstrate that corrosion by chlorine ions occurs on both Ag_3Al and Ag_2Al, and no corrosion is found on Ag or Al sample. In the following paragraphs, the corrosion mechanisms of Ag_3Al and Ag_2Al will be presented, following by a proposed corrosion model.

Figure 5a displays the microstructures of the corrosion region and corrosion-induced cracks in the Ag_3Al compound. Figure 5b shows an enlarged region. On the SEM images, red dots marked 1–12 indicate the EDX analysis location on the corrosion region. The resulting element compositions are listed in a table below. The microstructures consist of numerous submicron voids and cracks that were produced by the corrosion reactions. EDX analysis picked up element Cl in the corrosion region and in the vicinity of the cracks. It is interesting to observe that the corrosion-induced cracks propagate through the dark corrosion region and extend into the Ag_3Al compound. Moisture and Cl^- ions could penetrate through the cracks and voids in the corrosion region and accelerate the corrosion

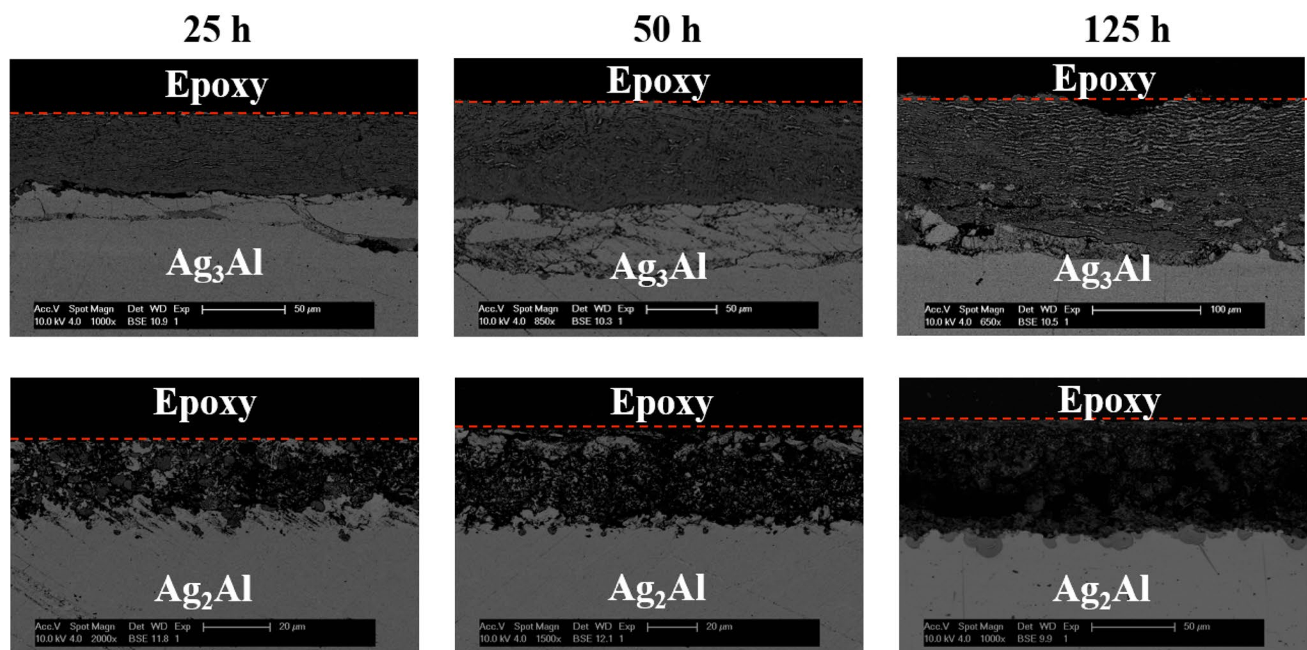

Fig. 3 The cross-sectional SEM back-scattered electron images of the Ag_3Al and Ag_2Al compounds molded in epoxy molding compounds after HAST for 25, 50, and 125 h

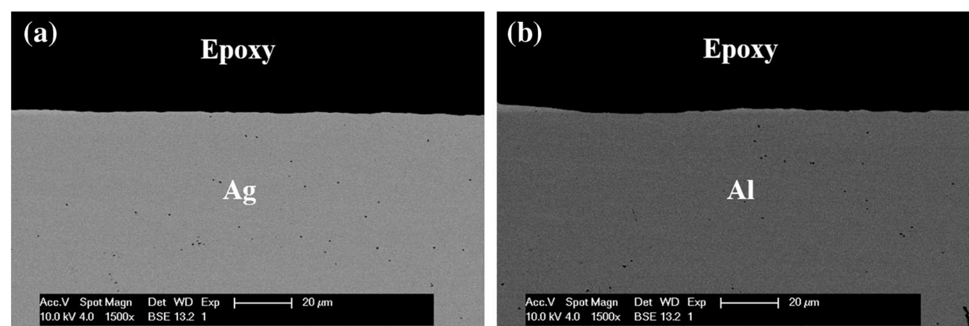

Fig. 4 The cross-sectional SEM back-scattered electron images of **a** Ag and **b** Al molded in epoxy molding compounds after HAST for 125 h

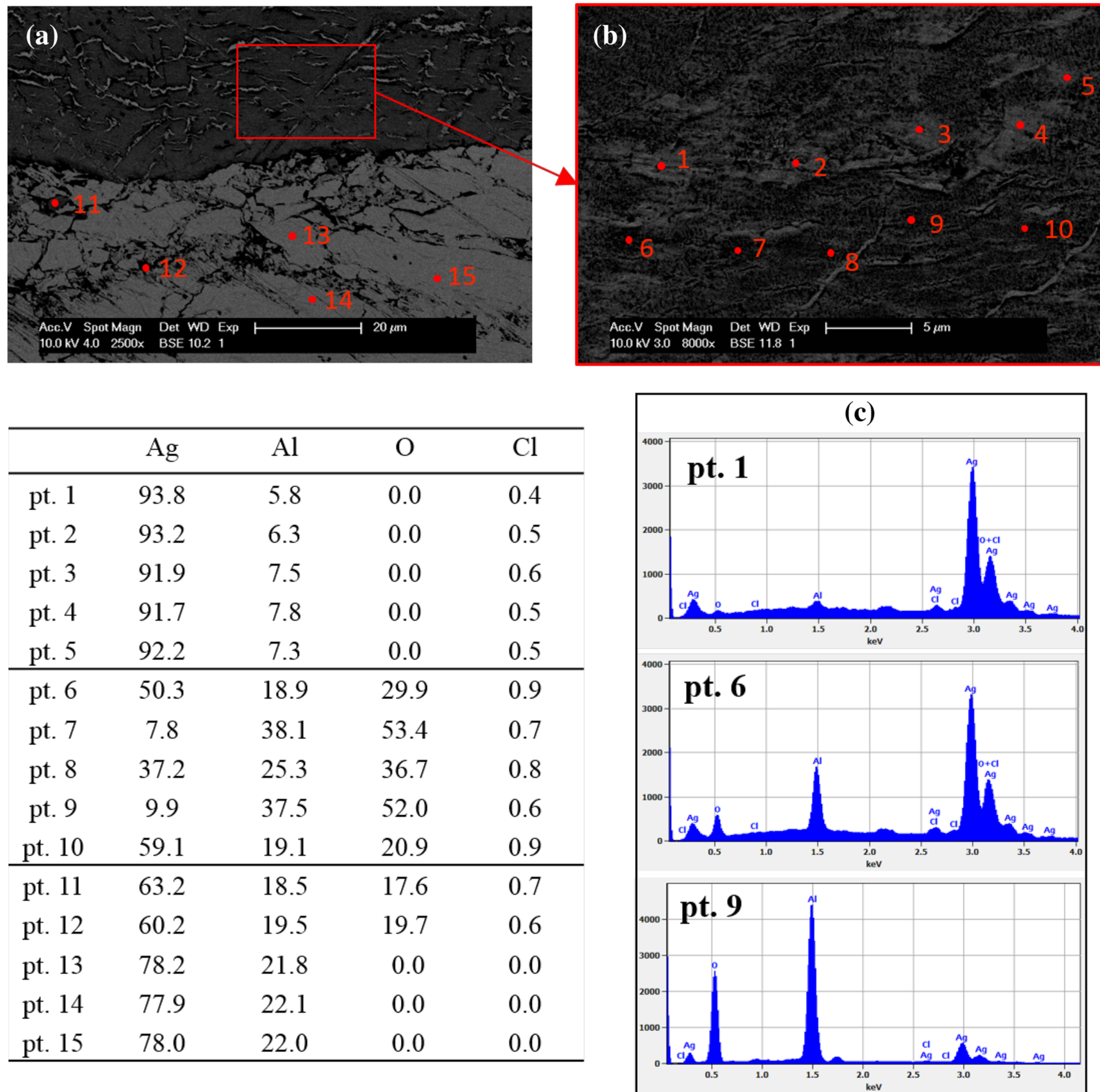

	Ag	Al	O	Cl
pt. 1	93.8	5.8	0.0	0.4
pt. 2	93.2	6.3	0.0	0.5
pt. 3	91.9	7.5	0.0	0.6
pt. 4	91.7	7.8	0.0	0.5
pt. 5	92.2	7.3	0.0	0.5
pt. 6	50.3	18.9	29.9	0.9
pt. 7	7.8	38.1	53.4	0.7
pt. 8	37.2	25.3	36.7	0.8
pt. 9	9.9	37.5	52.0	0.6
pt. 10	59.1	19.1	20.9	0.9
pt. 11	63.2	18.5	17.6	0.7
pt. 12	60.2	19.5	19.7	0.6
pt. 13	78.2	21.8	0.0	0.0
pt. 14	77.9	22.1	0.0	0.0
pt. 15	78.0	22.0	0.0	0.0

Fig. 5 **a** The SEM back-scattered electron images and EDX composition analysis of the corroded Ag_3Al compound after 50-h HAST. **b** The SEM image of an enlarged corrosion region. *Red dots* marked by 1–12 indicate the EDX analysis locations. The resulting element compositions are listed in the table. **c** The EDX energy spectra of representative analysis locations. (Color figure online)

propagation into the Ag_3Al compound. The dispersed bright phase in the porous corrosion region was identified as Ag precipitates, as shown in pt. 1–5. On the dark regions, EDX analysis exhibits significant variations in Ag, Al, and O element contents, as shown in pt. 6–10. The EDX energy spectra of representative analysis locations are displayed in Fig. 5c. At randomly selected locations on dark regions, such as pt. 7 and 9, EDX analysis detected dominant Al and O signals. Since silver oxide is thermodynamically unstable, the Al and O signals could come from aluminum oxide. It is probable that the corrosion reaction caused by moisture and Cl^- ions converts the Ag_3Al compound into corroded region consisting of aluminum oxide and dispersed Ag precipitates.

Figure 6 shows the corrosion region in a Ag_2Al sample and the EDX results after the same HAST conditions. It is seen that there are large number of voids in the corrosion region, but there are no propagating cracks as observed on the corroded Ag_3Al in Fig. 5. The high magnification image, Fig. 6b, exhibits a seemingly random distribution of granular dark phase and irregular bright phase. EDX analysis identified the dispersed bright phase as Ag precipitates with similar compositions that on the corroded Ag_3Al. The dark region was identified as mixed phase containing Ag, Al, O and Cl. Higher Al and O contents were detected in the dark corrosion region of Ag_2Al as compared to Ag_3Al, which could possibly be attributed to higher proportion of aluminum oxide product in the corroded Ag_2Al. Figure 7

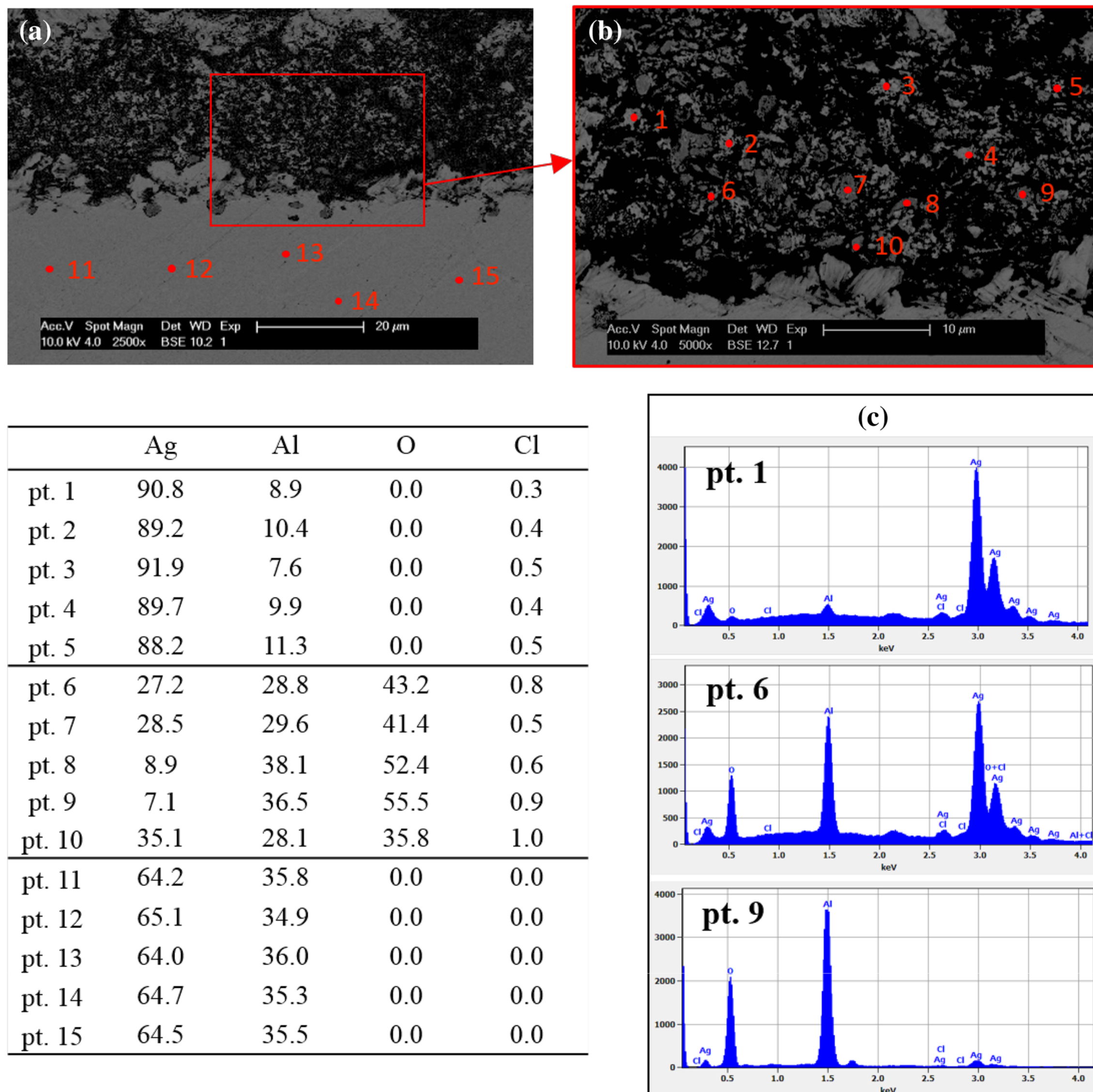

	Ag	Al	O	Cl
pt. 1	90.8	8.9	0.0	0.3
pt. 2	89.2	10.4	0.0	0.4
pt. 3	91.9	7.6	0.0	0.5
pt. 4	89.7	9.9	0.0	0.4
pt. 5	88.2	11.3	0.0	0.5
pt. 6	27.2	28.8	43.2	0.8
pt. 7	28.5	29.6	41.4	0.5
pt. 8	8.9	38.1	52.4	0.6
pt. 9	7.1	36.5	55.5	0.9
pt. 10	35.1	28.1	35.8	1.0
pt. 11	64.2	35.8	0.0	0.0
pt. 12	65.1	34.9	0.0	0.0
pt. 13	64.0	36.0	0.0	0.0
pt. 14	64.7	35.3	0.0	0.0
pt. 15	64.5	35.5	0.0	0.0

Fig. 6 **a** The SEM back-scattered electron images and EDX composition analysis of the corroded Ag_2Al compound after 50-h HAST. **b** The SEM image of an enlarged corrosion region. *Red dots* marked by 1–12 indicate the EDX analysis location. The resulting element compositions are listed in the table. **c** The EDX energy spectrum of the representative composition analysis points. (Color figure online)

displays the result of EDX elemental mapping of Ag, Al, O, and Cl element on the corroded Ag_2Al under high magnification. It is interesting to observe that Cl distributed in the irregular black region around the voids and cracks on the corroded Ag_2Al. Since the EDX mapping reveals complementary distribution of Cl and Ag, the relatively Cl-rich region is most likely attributed to the formation of aluminum chloride during the corrosion reaction. As aluminum chloride is considered chemically unstable, it can be readily hydrolyzed by moisture or consequently changed into aluminum oxide, leading to micro-void and micro-crack formation in the corrosion region.

Figure 8 depicts the corrosion layer thickness on Ag_3Al and Ag_2Al disks, respectively, molded in EMC after HAST for different times. For both Ag_3Al and Ag_2Al, linear regression analysis was used to confirm the linear relationship between the thickness of the corroded layer and the reaction time. The standard deviation and the calculated fitting curve are shown in the graph. The adjusted R-squared values for both linear models are above 0.98 (0.99 for Ag_3Al and 0.98 for Ag_2Al), suggesting a good fit with the experimental data. The thickness versus time curves clearly indicates that Ag_3Al experiences significantly higher corrosion rate compared to Ag_2Al. The linear growth curve implies that the corrosion rate is not diffusion-limited, but rather is reaction rate-limited. The curves can be described by

$$\mathbf{x} = \mathbf{kt}$$

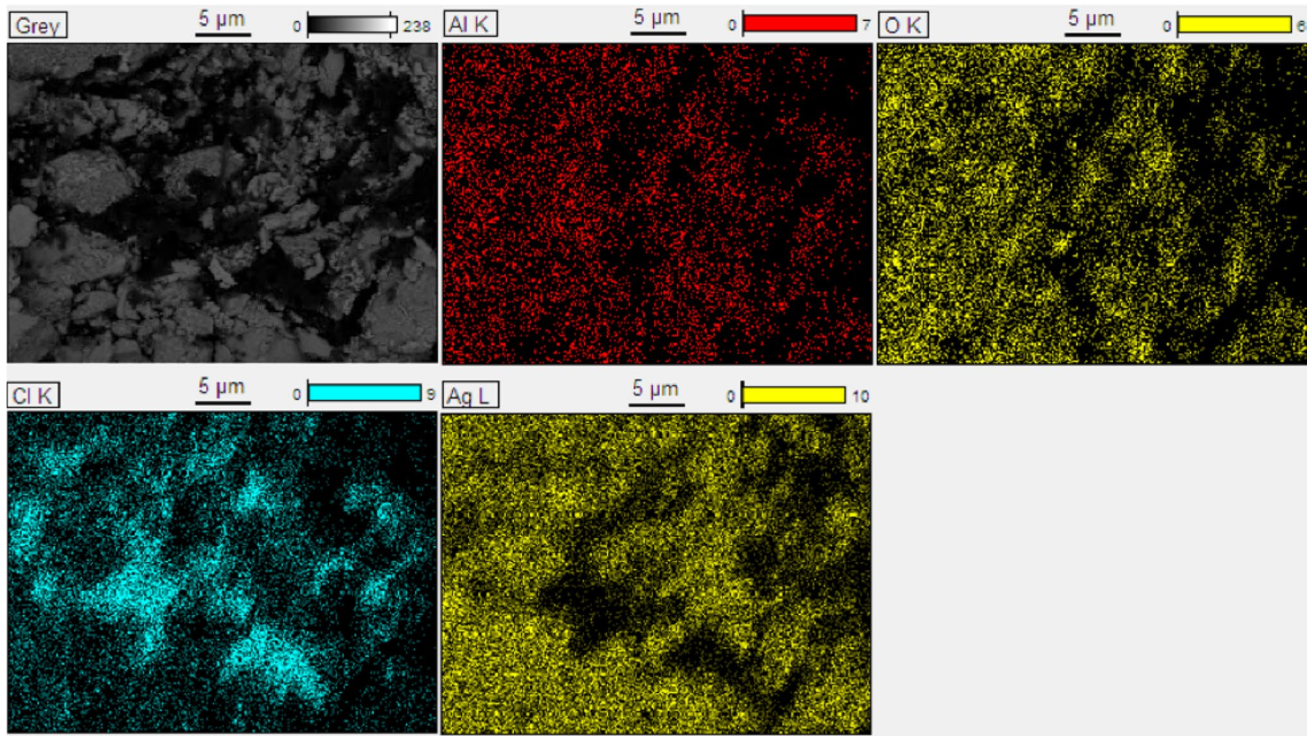

Fig. 7 SEM images and EDX elemental mappings of Ag, Al, O, and Cl elements on the corrosion region of Ag_2Al

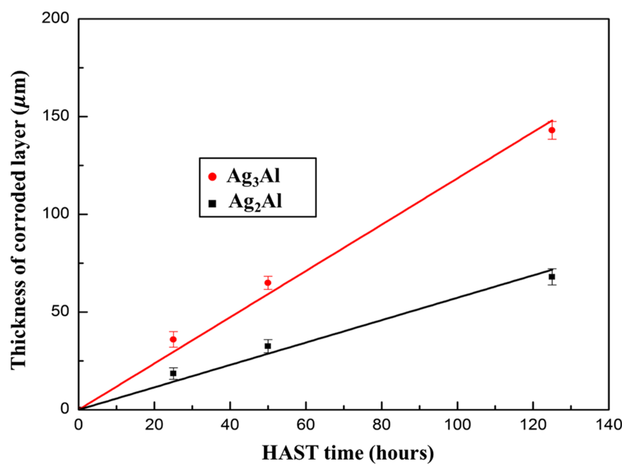

Fig. 8 Corrosion layer thickness versus HAST time on bulk Ag_3Al and Ag_2Al disks molded in epoxy molding compound containing chlorine ions

where **x** is the corrosion thickness, **k** is the corrosion rate constant, and **t** is the reaction time. It is seen that the corrosion rate on Ag_3Al is approximately twice the rate on Ag_2Al. This means that Ag_2Al is more resistant to corrosion than Ag_3Al by a factor of 2. Thus, Ag_3Al compound is the weak region in Ag–Al joints due to its high corrosion rate. The corrosion test method reported in this paper can potentially become a test standard for devices molded in EMC that go through various reliability tests.

According to the results shown above, after HAST, corrosion occurs on both Ag_3Al and Ag_2Al but not on Ag and Al. The relatively Cl-rich region detected around the voids and cracks in the corroded Ag2Al could indicate the formation of aluminum chloride as the intermediate product. After corrosion reaction, Ag_3Al and Ag_2Al compounds disintegrate into the corrosion region consisting of aluminum oxide and dispersed Ag precipitates. Based on the microstructural characterization, a corrosion model is proposed as a sequence of reactions below. The corrosion model is also schematically illustrated in Fig. 9.

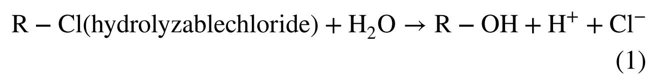

$$R - Cl(\text{hydrolyzablechloride}) + H_2O \rightarrow R - OH + H^+ + Cl^- \quad (1)$$

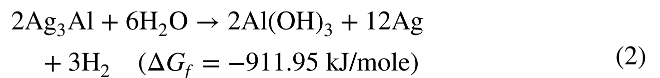

$$2Ag_3Al + 6H_2O \rightarrow 2Al(OH)_3 + 12Ag + 3H_2 \quad (\Delta G_f = -911.95\ \text{kJ/mole}) \quad (2)$$

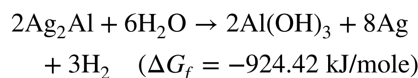

$$2Ag_2Al + 6H_2O \rightarrow 2Al(OH)_3 + 8Ag + 3H_2 \quad (\Delta G_f = -924.42\ \text{kJ/mole})$$

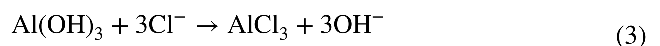

$$Al(OH)_3 + 3Cl^- \rightarrow AlCl_3 + 3OH^- \quad (3)$$

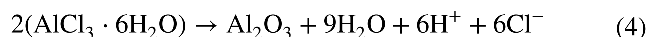

$$2(AlCl_3 \cdot 6H_2O) \rightarrow Al_2O_3 + 9H_2O + 6H^+ + 6Cl^- \quad (4)$$

The Ag–Al IMC corrosion occurs specifically in the presence of moisture and chlorine ion. Reaction (1)

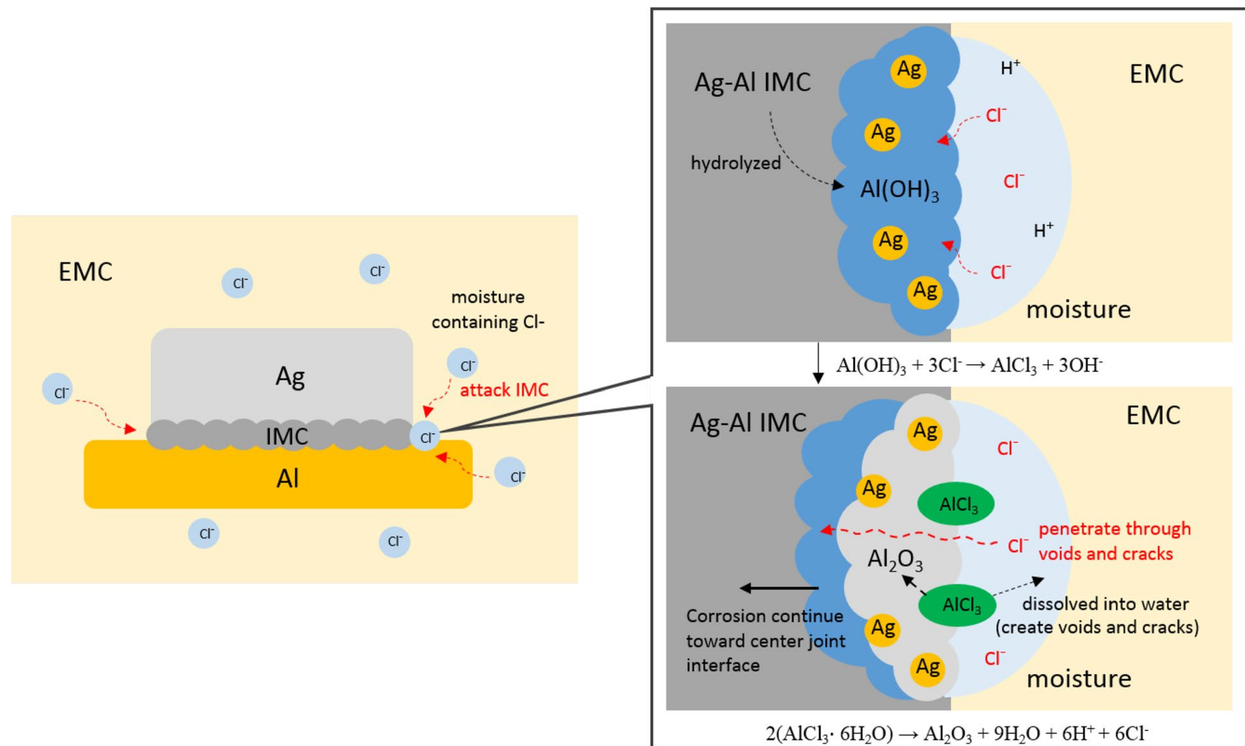

Fig. 9 Schematic illustration of proposed corrosion model of the Ag–Al IMC in chlorine-containing EMC under HAST

describes the production of chlorine ions in the EMC. Under HAST, moisture can penetrate through the EMC and react with hydrolyzable chloride to release Cl^- ions and hydrogen ion (H^+) [24]. Moisture and Cl^- ions can diffuse to the Ag/Al joint interface and initiate the IMC corrosion. In moisture environment, Ag_3Al and Ag_2Al IMC can be hydrolyzed and transformed into aluminum hydroxide ($Al(OH)_3$), as given in reaction (2). This reaction also forms H_2 gas as a by-product. The out-gassing of H_2 gas can lead to micro-crack formation in the corrosion region. As the moisture and Cl^- ion diffuse to the IMC region, $Al(OH)_3$ can easily react with Cl^- ions and produce aluminum chloride ($AlCl_3$) [26, 27], as shown in reaction (3). As aluminum chloride is chemically unstable, it can be readily hydrolyzed by moisture or transformed into aluminum oxide. In the temperature range of 100 to 200 °C, $AlCl_3$ hydrolyzes into $AlCl_3{\cdot}6H_2O$ octahedral complex and decomposes into aluminum oxide (Al_2O_3) [28], as shown in reaction (4). The hydrolyzation of $AlCl_3$ can lead to micro-void and micro-crack formation in the corrosion region.

In the corrosion mechanism of IMC, the level of moisture and Cl^- ions in the EMC is a dominant factor. As moisture and Cl^- ions diffuse through the EMC and initiate the IMC corrosion, aluminum chloride can form as an intermediate product and can be immediately hydrolyzed into aluminum oxide. This hydrolyzation reaction also releases additional Cl^- ions into the moisture environment, which can accelerate the repetitive reduction and oxidation reactions, from reactions (2) to (4). The formation of voids, cracks, and oxides in the corrosion region will weaken the Ag–Al joint and increase its electrical resistance. Thus, restricting the concentrations of moisture and Cl^- ions in the EMC is extremely important in keeping the quality of Ag–Al joints. Formulation of EMC with low chlorine level and low moisture permeability is a solution. Since corrosion occurs only in IMC region, reducing Ag–Al IMC growth is another possible solution. For Ag–Al wire bonds, adding some elements to Ag wires might suppress the IMC growth. Recently, Au and Pd elements have been added to produce Ag alloy wires. It is still not clear if these elements suppress the IMC growth.

In conclusion, the corrosion reactions of Ag–Al joints in EMC under HAST were investigated in this study. Results show that the corrosion mainly occurs in the IMC region. In the real Ag–Al wire bonding application, bonding parameters could affect the grain size of Ag–Al IMC and the morphology of Ag/Al bonding interface, which could potentially influence the IMC corrosion rate. By establishing the corrosion experiment with bulk Ag–Al intermetallic compounds, this research quantifies the intrinsic reactivity of Ag_2Al and Ag_3Al with moisture and Cl- and provides possible directions for securing the Ag–Al bonding reliability. Further study on the corrosion behavior of Ag–Al wire bonding will be conducted in our future research.

4 Summary

In this study, the reactions of Ag–Al joints and bulk Ag–Al intermetallic compounds with chlorine-containing EMC under HAST were studied. The results show that corrosion induced by moisture and Cl^- ions occurs on both Ag_3Al and Ag_2Al. No corrosion is detected on Ag or Al samples. The corrosion rates of Ag_3Al and Ag_2Al were measured, respectively, by a quantitative test method. The rates are linear versus time, indicating that the corrosion is reaction-controlled rather than diffusion-controlled. Corrosion rate on Ag_3Al is twice of that on Ag_2Al. Microstructures, phases, and compositions of corroded regions in Ag_3Al and Ag_2Al were examined in details. Bulk Ag_3Al and Ag_2Al compounds were broken down by moisture and Cl^- ions and disintegrated into corrosion regions consisting of aluminum oxide pieces and dispersed Ag precipitates with voids and cracks. A corrosion model was proposed to establish the chemical reactions of Ag_3Al and Ag_2Al with moisture and Cl^- ions in EMC. It is clear that moisture and Cl^- ions are the key ingredients that cause the corrosion. Accordingly, to counter the corrosion, the moisture diffusion through the package and/or the Cl^- ion concentration in EMC must be controlled and reduced. This is the direction discovered in this research to reduce Ag–Al wire-bond corrosion.

Acknowledgements SEM/EDX and XRD analysis were performed at the UC Irvine Materials Research Institute (IMRI).

References

1. C. Harper, *Electronic Packaging and Interconnection Handbook*, (McGraw-Hill, New York, 2004)
2. E.R.R. Tummala, E.J. Rymaszewski, *Microelectronics Packaging Handbook*, (Springer, New York, 1997)
3. G.G. Harman, *Wire Bonding in Microelectronics*, (McGraw-Hill, New York, 2010)
4. J. Cho, H. Jeong, J. Moon, S. Yoo, J. Seo, S. Lee, S. Ha, E. Her, S. Kang and K. Oh, Thermal reliability & IMC behavior of low cost alternative Au–Ag–Pd wire bonds to Al metallization, in *2009 IEEE 59th Electronic Components and Technology Conference* (*ECTC*) (2009), pp. 1569–1573
5. C.L. Gan, U. Hashim, Evolutions of bonding wires used in semiconductor electronics: perspective over 25 years. J. Mater. Sci. **26**(7), 4412–4424 (2015)
6. Z. Zhong, Overview of wire bonding using copper wire or insulated wire. Microelectron. Reliab. **51**(1), 4–12 (2011)
7. B.K. Appelt, A. Tseng, C. Chen, Y. Lai, Fine pitch copper wire bonding in high volume production. Microelectron. Reliab. **51**(1), 13–20 (2011)
8. C. Yu, C. Chan, L. Chan, K. Hsieh, Cu wire bond microstructure analysis and failure mechanism. Microelectron. Reliab. **51**(1), 119–124 (2011)
9. R. Guo, T. Hang, D. Mao, M. Li, K. Qian, Z. Lv, H. Chiu, Behavior of intermetallics formation and evolution in Ag–8Au–3Pd alloy wire bonds. J. Alloys Compd. **588**, 622–627 (2014)
10. T. Chuang, C. Tsai, H. Wang, C. Chang, C. Chuang, J. Lee, H. Tsai, Effects of annealing twins on the grain growth and mechanical properties of Ag–8Au–3Pd bonding wires, J. Electron. Mater. 41(11), 3215–3222 (2012)
11. C. Cheng, H. Hsiao, S. Chu, Y. Shieh, C. Sun, C. Peng, Low cost silver alloy wire bonding with excellent reliability performance. in *2013 IEEE 63rd Electronic Components and Technology Conference* (*ECTC*) (2013), pp. 1569–1573
12. H. Kim, J.Y. Lee, K. Paik, K. Koh, J. Won, S. Choe, J. Lee, J. Moon, Y. Park, Effects of Cu/Al intermetallic compound (IMC) on copper wire and aluminum pad bondability. IEEE Trans. Compon. Packag. Technol. **26**(2), 367–374 (2003)
13. Y. C. Jang, S. Y. Park, H. D. Kim, Y. C. Ko, K. W. Koo, M. R. Choi, H. G. Kim, N. K. Cho, I.T. Kang, J.H. Yee, Study of intermetallic compound growth and failure mechanisms in long term reliability of silver bonding wire, in *2014 IEEE 16th Electronics Packaging Technology Conference* (*EPTC*) (2014), pp. 704–708
14. J. Tsai, A. Lan, D. Jiang, L. W. Wu, J. Huang, J. Hong, Ag alloy wire characteristic and benefits, in *2014 IEEE 64th Electronic Components and Technology Conference* (*ECTC*) (2014), pp. 1533–1538
15. L.J. Kai, L.Y. Hung, L.W. Wu, M.Y. Chiang, D.S. Jiang, C. Huang, Y. P. Wang, Silver alloy wire bonding, in *2012 IEEE 62nd Electronic Components and Technology Conference* (*ECTC*) (2012), pp. 1163–1168
16. J. Xi, N. Mendoza, K. Chen, T. Yang, E. Reyes, S. Bezuk, J. Lin, S. Ke, E. Chen, Evaluation of Ag wire reliability on fine pitch wire bonding, in *2015 IEEE 65th Electronic Components and Technology Conference* (*ECTC*) (2015), pp. 1392–1395
17. A. McAlister, The Ag–Al (silver–aluminum) system. Bull. Alloy Phase Diagr. **8**(6), 526–533 (1987)
18. S. Lim, P. Rossiter, J. Tibballs, Assessment of the Al–Ag binary phase diagram. Calphad **19**(2), 131–141 (1995)
19. Y. Chiu, T. Chiang, P. Yang, L. Huang, C. Hung, S. Uegaki, K. Lin, The corrosion behavior of Ag alloy wire bond on Al pad in molding compounds of various chlorine contents under biased-HAST, in *Electronics Packaging* (*ICEP*), 2016 international conference (2016), pp. 497–501
20. M. Lue, C. Huang, S. Huang, K. Hsieh, Bromine-and chlorine-induced degradation of gold-aluminum bonds, J. Electron. Mater. **33**(10), 1111–1117 (2004)
21. C.L. Gan, C. Francis, B.L. Chan, U. Hashim, Extended reliability of gold and copper ball bonds in microelectronic packaging. Gold Bull. **46**(2), 103–115 (2013)
22. P. Su, H. Seki, C. Ping, S. Zenbutsu, S. Itoh, L. Huang, N. Liao, B. Liu, C. Chen, W. Tai, An evaluation of effects of molding compound properties on reliability of Cu wire components, in *2011 IEEE 61st Electronic Components and Technology Conference* (*ECTC*) (2011), pp. 363–369
23. T. Uno, Bond reliability under humid environment for coated copper wire and bare copper wire. Microelectron. Reliab. **51**(1), 148–156 (2011)
24. C. May, *Epoxy Resins: Chemistry and Technology* (CRC Press, Boca Raton, 1987)
25. H. B. Fan, E. K. Chan, C. K. Wong, M. M. Yuen, Investigation of moisture diffusion in electronic packages by molecular dynamics simulation. J. Adhes. Sci. Technol. **20**(16), 1937–1947 (2006)
26. S.K. Prasad, *Advanced Wire Bond Interconnection Technology*, (Springer, New York, 2004)
27. B.D. Craig, *Fundamental Aspects of Corrosion Films in Corrosion Science*, (Springer, New York, 2013)
28. H.K. Farag, F. Endres, Studies on the synthesis of nano-alumina in air and water stable ionic liquids. J. Mater. Chem. **18**(4), 442–449 (2008)